Solid-State NMR Study of Charge-Transfer Interactions in Polymer Blends

Alexandra Simmons and Almeria Natansohn*

Department of Chemistry, Queen's University, Kingston, Ontario K7L 3N6, Canada

Received November 27, 1990; Revised Manuscript Received January 23, 1991

ABSTRACT: Polymer blends containing electron donor (*N*-ethylcarbazol-3-yl)methyl methacrylate (NECMM) and electron acceptor 2-[(3,5-dinitrobenzoyl)oxy]ethyl methacrylate (DNBEM) moieties were prepared and analyzed by differential scanning calorimetry (DSC) and solid-state nuclear magnetic resonance (NMR). The number of inter- vs intramolecular charge-transfer (CT) interactions was varied by preparing blends of polydonor with polyacceptor, as well as blends containing a homopolymer and an acceptor–donor copolymer. The blends were one phase for NECMM contents greater than 35 mol %. At lower donor contents, two phases with different amounts of CT complexation were shown to exist. DSC, via T_g, and NMR, via $T_{1\rho}(^1H)$, indicate that CT interactions result in restricted mobility and reduced free volume and interatomic distances in the bulk polymer blends. Intermolecular CT complexes are decomplexed on heating above 185 °C, and two phases, composed of only one blend component, are formed. A chemical shift investigation of CT in small molecule analogues suggests that the complex has an asymmetrical structure.

Introduction

Nonbonding interactions play an important role in determining the physical properties of bulk polymers. In addition, they provide the driving force for miscibility in many macromolecular systems. It is clear that an understanding of such interactions at the molecular level is necessary in order to determine the mechanism of self-organization in high molecular weight systems and to be able to design materials with desirable characteristics.

Even a solid sample of a polymer composed of a single type of repeating unit is a complex and spatially inhomogeneous system that may present a variety of analytical problems. Characterization of polymer blends in which several components and phases are present is consequently more challenging.

One way to simplify the analysis of interactions in polymers is to study the corresponding low molecular weight systems. This approach has met with considerable success in some areas. One recent example involved determination of heats of mixing and interaction parameters of model compounds by calorimetry and allowed the prediction of miscibility windows in blends of poly(vinyl chloride) with ethylene–vinyl acetate copolymers.[1] In another instance, infrared spectroscopy confirmed the presence of interactions between models of styrene, maleic anhydride, and acrylonitrile and increased understanding of miscibility in some blends of styrene-*co*-maleic anhydride with styrene-*co*-acrylonitrile.[2]

Few techniques are available that can probe the molecular level of bulk polymers. By using solid-state nuclear magnetic resonance (NMR) and combining chemical shift and relaxation studies, one can investigate the chemical environment and molecular motion of specific sites on a polymer chain.

Solid-state NMR has been used only rarely to study the effect of nonbonding interactions on the chemical shift of models for polymeric systems. However, the appearance of *covalent* bonding during the curing of poly(styrylpyridine)[3] and epoxy[4] resin precursors has been investigated. ^{13}C CPMAS NMR has been used to observe the effects of nonbonding interactions in small molecule systems unrelated to polymers. Guest–host interactions in poly-*tert*-butyl(calix[4]arene)/toluene clathrates[5] and Dianin's compound clathrates[6] bring about chemical shift changes, while electron transfer from hexamethylbenzene to a series of acceptors results in a downfield shift of the donor aromatic carbons.[7]

In bulk macromolecular systems, the difference in chemical shift due to nonbonding interactions is often smaller than the line width. In a few cases of polymer/polymer or polymer/small molecule blends, some effect has been detected. The carbonyl carbons in polybenzimidazole/polyimide blends[8] and blends of poly(ethylene oxide) with resorcinol[9] are broadened and shifted due to hydrogen bonding. Upfield shifts of some carbons of 2,4,7-trinitro-9-fluorenone or 2,4,5,7-tetranitro-9-fluorenone in complexes with poly(*N*-vinylcarbazole) have been observed.[10]

Proton $T_{1\rho}$ has been successfully used to probe molecular mixing in many polymer blends. At the time of writing this paper, these include polystyrene/polystyrene–polybutadiene block copolymer blends,[11] polystyrene with poly(phenylene oxide),[12] poly(vinylidene fluoride) with poly(methyl methacrylate),[13,14] poly(2- or 4-methylstyrene)/poly(2,6-dimethylphenylene oxide),[15] Bisphenol A polycarbonate and poly(ethylene terephthalate),[16] polystyrene/poly(vinyl methyl ether),[17] polymethacrylates with poly(vinyl chloride),[18] poly(phenylene sulfide)/poly(ether sulfone),[19] lignin with polyurethane,[20] poly(ether sulfone)/polyimide,[21] polybenzimidazole/polyimide,[8] poly(ethylene oxide)/poly(methyl methacrylate),[22,23] and isotactic with syndiotactic poly(methyl methacrylate).[24] It has also proven useful in polymer/small molecule systems[25,26] and glass-filled nylon composites.[27]

In our laboratory, we combine solid-state NMR with differential scanning calorimetry (DSC) in an attempt to establish a correlation between microscopic and macroscopic behavior. One of the aims of our research is to understand the nature and effects of charge-transfer (CT) interactions in polymers. An ongoing study involves polymers containing (*N*-ethylcarbazol-3-yl)methyl methacrylate (NECMM), an electron donor, and/or 2-[(3,5-dinitrobenzoyl)oxy]ethyl methacrylate (DNBEM), an electron acceptor. Preliminary results on the use of solid-state NMR to study CT interactions in a single NECMM–DNBEM copolymer, and one pNECMM/pDNBEM blend and some small molecule analogues have appeared.[28] We recently reported on the application of DSC and solid-state NMR to study CT interactions in copolymers of

0024-9297/91/2224-3651$02.50/0

NECMM with DNBEM.[29] The present work describes a continuation of the investigation to include blends of pNECMM with pDNBEM, where only intermolecular interactions are present, as well as homopolymer/copolymer blends.

Experimental Section

Materials. Monomers and homo- and copolymers, as well as small molecule analogues, were prepared as described in the literature.[29-33] Polymer blends were obtained by mixing 1% (w/v) solutions of the polymers in boiling THF, followed by precipitation into methanol. All samples were dried in vacuo for several days at ~70 °C. A portion of each blend was heated in vacuo to 195 °C, held there for 15 min, and then quenched in liquid nitrogen to retain the morphology present. These samples are referred to as "decomplexed" throughout this work. Charge-transfer complexes of the low molecular weight analogues were made by dissolving the components in hot methanol at a level of 2.5% (w/v), mixing the solutions, and allowing the complex to crystallize out on cooling.

Analysis. The purity of all intermediates, monomers, small molecule analogues, and homopolymers, as well as the composition of copolymers and small molecule complexes, was confirmed by ^{1}H NMR in $CDCl_3$, DMSO-d_6, or a mixture of $CDCl_3$ and DMSO-d_6. Spectra were obtained on a Bruker AM-400 spectrometer.

Molecular weights were determined by gel permeation chromatography (GPC) using a Waters Associates liquid chromatograph equipped with a Model 440 absorbance detector and a Model R401 differential refractometer. A flow rate of 1.0 mL/min was used, and samples were dissolved in THF at a concentration of 0.2–0.5 wt %. Peak molecular weights were determined by comparing retention times in μ-Styragel columns to those of standard polystyrene samples.

Glass transition temperature, T_g, was measured by DSC on a Mettler TA3000 system at a scanning rate of 20 °C/min. In order to ensure reproducibility, samples were subjected to four heating scans in succession over the temperature ranges 40–170, 40–170, 40–225, and 40–225 °C. T_g was taken as the peak of the first derivative curve.

^{13}C solid-state NMR spectra were collected with cross polarization, magic angle spinning, and dipolar decoupling (CP-MAS/DD). The proton spin–lattice relaxation time constant in the rotating frame, $T_{1\rho}(^1H)$, was measured by using a spin-locking pulse sequence with a 90° pulse of 3.8 μs, a 10-s delay between pulses, and a variable contact time from 0.25 to 50 ms.[12] Dipolar dephased spectra in which a contact time of 4–5 ms was followed by a 50–60-μs dephasing time were also acquired.[34]

Results and Discussion

Chemical Shift Studies. The chemical shift is correlated with the electron density at a given nucleus and can therefore yield information about its immediate chemical environment. Since CT interactions involve the transfer of electron density from the donor to the acceptor, we expect chemical shift changes to occur upon complexation. One might predict that the increased electron density on the acceptor would shift some peaks upfield, whereas the loss of electron density from the donor could result in a downfield shift.

The ^{13}C spectra of the donor homopolymer (pNECMM), the acceptor homopolymer (pDNBEM), and a 50:50 (mol/mol) blend of the two obtained under CP-MAS/DD conditions are shown in Figure 1, along with the chemical formula of each repeat unit. It is apparent that there is considerable overlap between the two homopolymer spectra, which make any comparison with the blend spectra difficult.

Some spectral editing was attempted by inserting a short delay before the acquisition of the spectrum. During the delay, the decoupler is turned off, and the carbon magnetization is allowed to decay under the influence of the C–H dipolar coupling. Tightly coupled (e.g., protonated) carbons decay quickly and a spectrum of only nonprotonated (or weakly coupled very mobile) carbons is obtained under the appropriate conditions.[34] Then a spectrum of the protonated carbons can be obtained by difference.

The application of dipolar dephasing difference spectroscopy to the polymer blend did result in two sets of simpler spectra, which allowed us to confirm some assignments. However, significant chemical shift differences between the homopolymers and the blend were not observed. We believed this to be due to the extremely broad peaks as a result of the variety of conformations frozen into the polymeric system. Therefore, we decided to undertake an investigation of CT interactions between a pair of small molecules that are analogues of the donor and acceptor repeat units.

The molecules we chose to model our polymer repeat units were the acetate analogues of the methacrylate monomers, NECMA for the donor, DNBEA for the acceptor. Both the model donor and the model acceptor were white crystals, which formed colorless solutions in methanol. Mixing the solutions yielded a yellow solution, indicating formation of the charge-transfer complex (CTC). Upon cooling, bright yellow crystals formed, which were filtered and dried. Solution ^{1}H NMR of the product crystals showed that the 1:1 (mol/mol) NECMA/DNBEA complexes were formed irrespective of the initial donor to acceptor ratio. White crystals, assumed to be the pure donor or acceptor, appeared along with the yellow 1:1 complex crystals when large excesses of one component were used.

In a previous study of these model compounds and their CTC, the resonances of the acetates, but especially of the complex, were still fairly broad.[28] The CTC prepared by slow evaporation of THF from a NECMA/DNBEA mixture was less crystalline than that obtained by crystallization from methanol. Some changes in chemical shift were apparent, but they were not thoroughly investigated.

Figure 2 shows the ^{13}C spectra of the solid NECMA and DNBEA and the crystalline 1:1 CTC. Clearly, the line widths of the resonances are much smaller than for the corresponding polymers in Figure 1. The models were highly crystalline compounds, and evidence of this is seen in the spectra. Sometimes a single carbon will exhibit resonance at two slightly different frequencies because it experiences different environments due to packing in the crystal. For example, in the donor model NECMA, the 2, 7, and 6 aromatic carbons as well as the acetate methyl carbon resonances are all split into two peaks separated by 0.6–1.1 ppm, and the carbon in the 3 position on the ring is split into peaks nearly 2 ppm apart. Figures 3 and 4 show the dipolar dephased (nonprotonated) and difference (protonated) spectra, respectively, in the aromatic region (180–100 ppm). The assignments are also given in Figures 3 and 4, and any peaks that shift upon complexation are indicated. Table I lists the chemical shift values before and after complexation, as well as the differences.

It is possible to observe changes in chemical shift values on complexation for many resonances, although in some cases there is still too much overlap for unambiguous assignments to be made. The spectra are reproducible, but any shift of less than 0.5 ppm is probably insignificant. Any resonance that changed moved upfield. This is consistent with the effects seen in solution spectra of NECMA/DNBEA complexes.[33,35] At that time it was proposed that the formation of "sandwich"-type complexes would be accompanied by increased shielding due to the aromatic groups lying on top of each other in stacks. This effect appears to predominate, since even the donor resonances are shifted upfield, but to a lesser extent than those of the acceptor. For the DNBEA, the upfield shift

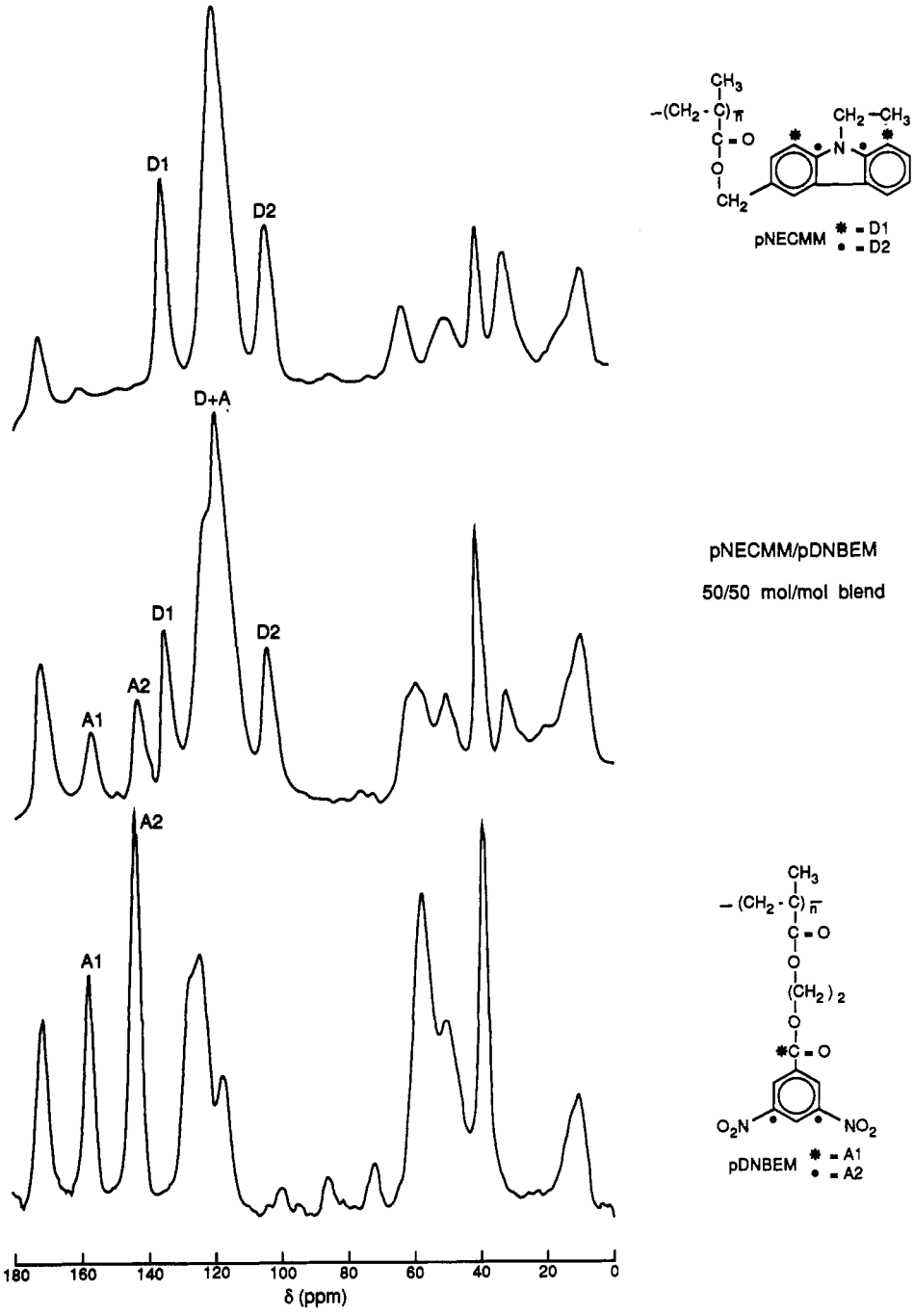

Figure 1. CP-MAS/DD ^{13}C spectra of (top to bottom) pNECMM, a 50:50 (mol/mol) blend of pNECMM and pDNBEM, and pDNBEM.

decreases in the order of carbons 3,5 > 1 > 4 > a > 2,6, while in NECMA, the greatest shifts are observed for carbons 8a and 9a, 1 and 8, and 4a and 5a. These shifts are consistent with the transfer of electron density from the NECMA to the DNBEA and indicate, as expected, that the changes are greatest on the aromatic ring of the DNBEA, especially the nitro carbons, and on the carbons in the pyrrole ring or adjacent to the N atom in NECMA.

Not all nominally equivalent carbons are affected the same way. The 3,5 (nitro) resonance of DNBEA splits into two peaks, one shifted by more than 5 ppm. The 8a and 9a, 4a and 5a, and 1 and 8 carbons of NECMA all present one component whose chemical shift does not change, and a second one of approximately equal intensity that moves upfield. The 3 carbon of the NECMA is not shifted, while it is not possible to assign with certainty the positions of the other aromatic resonances for NECMA in the CTC. It should be noted that the absence of any shift in the presence of the increased aromatic shielding actually indicates a decrease in electron density big enough to offset the ring current effect. Therefore it appears that one carbon out of each equivalent pair of NECMA carbons is involved in the donation of electron density to DNBEA upon formation of the CTC.

The above information is very useful in increasing our understanding of the structure of the CTC. Pearson et al.[36] reviewed the evidence that complexes of carbazole compounds in general might be either symmetric or asymmetric. Figure 5 shows the two possibilities for our system. The observations described above clearly favor the asymmetric complex. Such a complex would position the DNBEA molecule over only one aromatic ring of the NECMA, leaving the other nearly unaffected; it would also account for a difference in chemical shift of the 3 and 5 carbons in the DNBEA in the CTC. Therefore, by using a model system and performing dipolar dephasing difference spectroscopy in order to pinpoint the sites of electron transfer, it is possible to propose a structure for

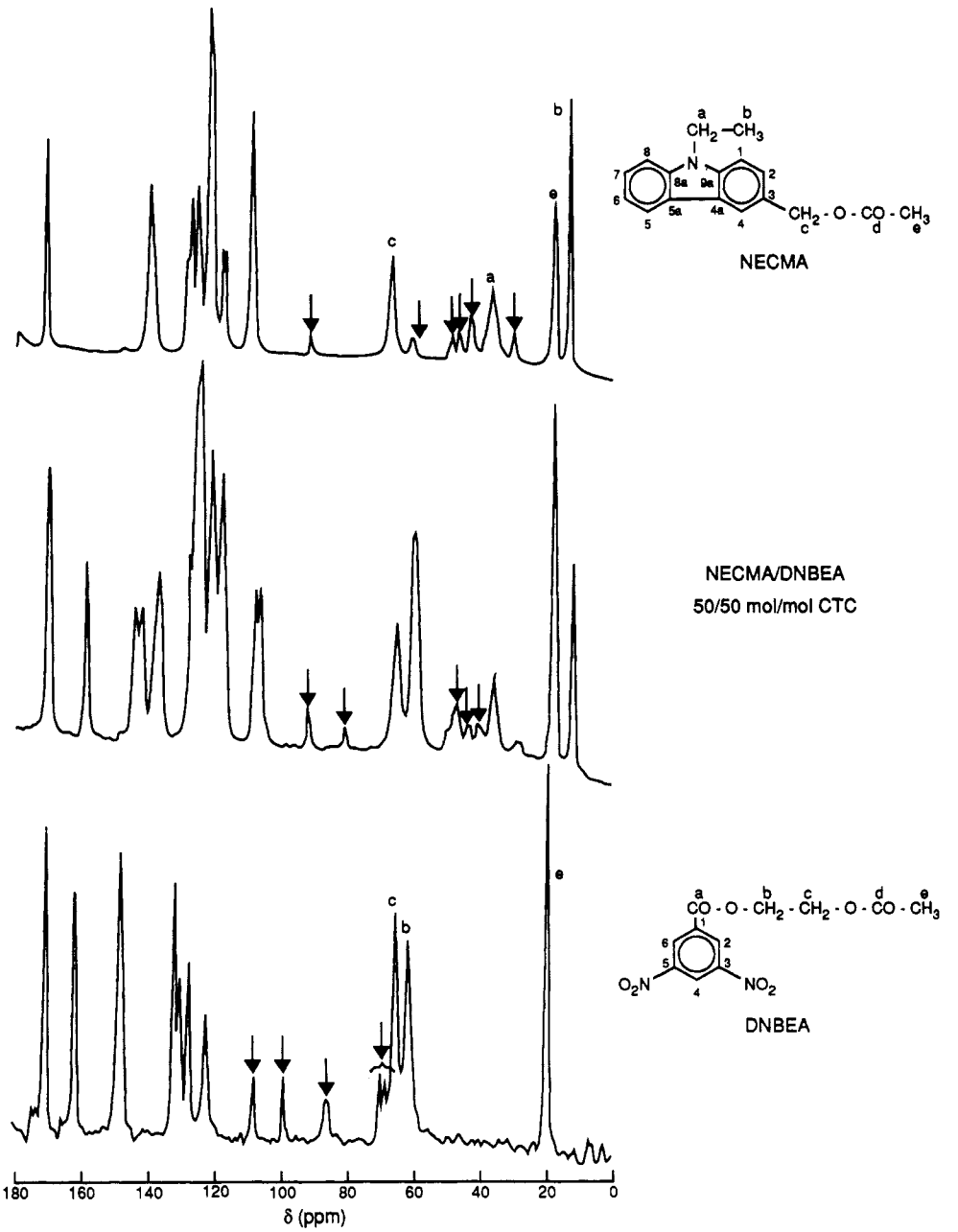

Figure 2. CP-MAS/DD ^{13}C spectra of small molecule analogues (top to bottom) NECMA; 50:50 (mol/mol) crystalline CTC of NECMA and DNBEA, and DNBEA. Arrows indicate spinning side bands.

the CTC in the solid state.

Homopolymer Blends. Both pNECMM, the polydonor, and pDNBEM, the polyacceptor, were obtained as white powders. GPC analysis revealed bi- or trimodal molecular weight distributions. Peak molecular weights, M_p, were around 28 000 for the pDNBEM and 85 000 for the pNECMM.

Mixing a THF solution of pNECMM with a solution of pDNBEM at room temperature resulted in the formation of an orange precipitate. Precipitation did not occur from boiling THF, so all blends were prepared by mixing boiling solutions of the homopolymers and continuing to stir for some time before the blends were precipitated in methanol. All the blends were orange, indicating that charge-transfer complexes were formed.

In an investigation of the properties of NECMM–DNBEM copolymers,[29] the effect of sample history was studied by comparing samples prepared by slow evaporation of THF with those prepared by precipitation, and by drying samples under different conditions. In contrast to the differences observed between precipitated and slow-evaporated copolymers, the blends made for the present study behaved similarly whether precipitated or slow evaporated. Perhaps this is due to the fact that under slow-evaporation conditions the blends precipitate, so they have the same properties as those precipitated directly. Consequently, only precipitated samples are considered in this work.

(a) Thermal Analysis. Prior study of some pNECMM/pDNBEM blends led to the conclusion that they form a unique system that can be used as a model for LCST in polymer blends.[37] At that time it was reported blends of any composition possessed a single T_g, and that as the temperature was increased to ~185 °C, an endotherm was detected. The presence of two T_gs in subsequent scans indicated that phase separation had taken place. Therefore, it was proposed that the endotherm reflected decomplexation of the donor and acceptor moieties.

The blends prepared for the present study show behavior similar to that described above. For example, Figure 6 shows the DSC data for a 50:50 (mol/mol) blend of

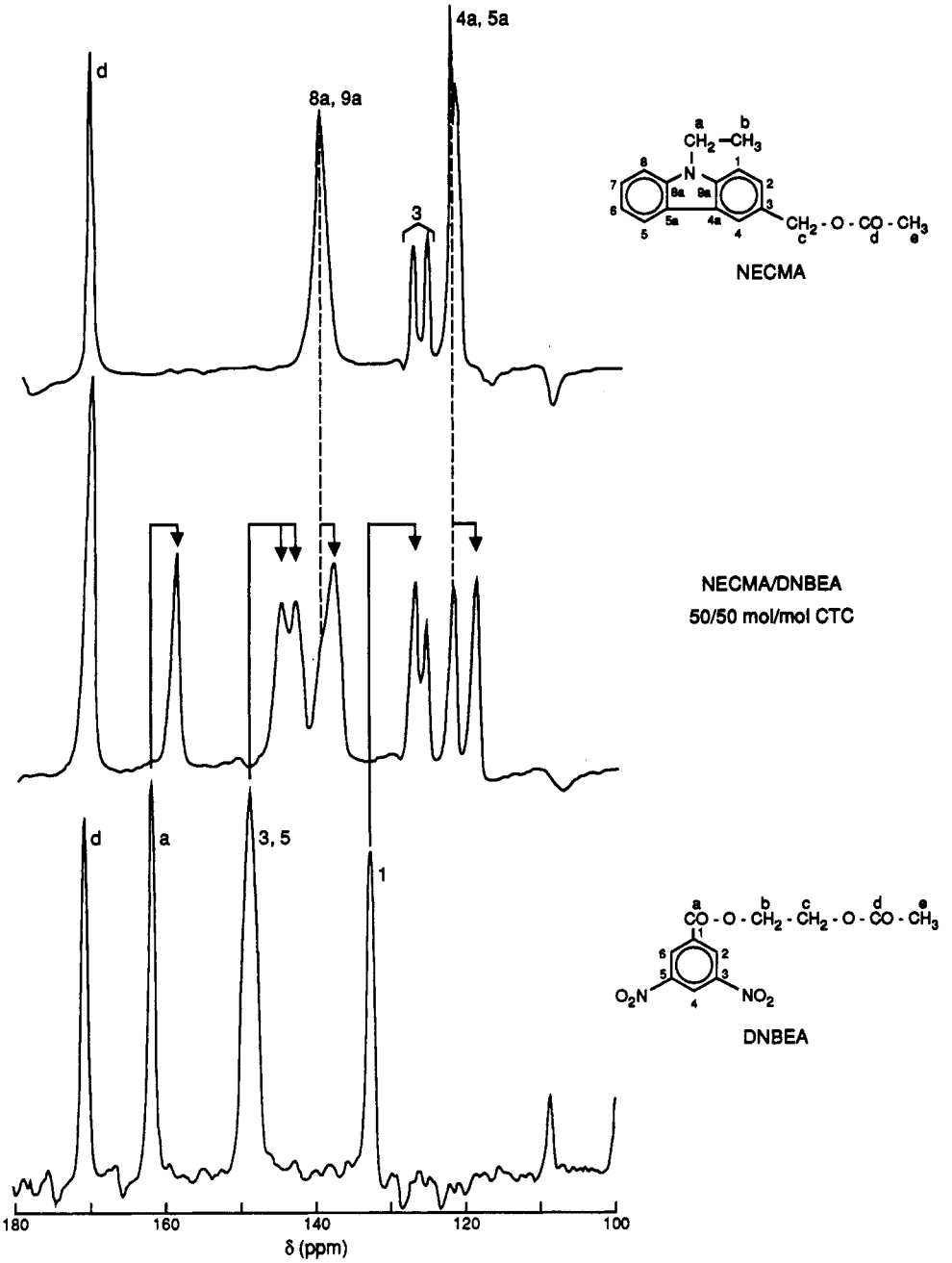

Figure 3. Aromatic region of dipolar dephased (dephasing time 60 μs) spectra of samples described in Figure 2. Arrows indicate shifts due to CTC formation.

pNECMM with pDNBEM before and after decomplexation, as well as the first derivative of the heat flow. When the T_g appears very broad, or the proportion of one component is below ~30 mol %, it is sometimes difficult to determine if the system has one or two T_gs. An analysis of the first derivative usually reduces the required interval between two T_gs for them to be detected as separate and also facilitates the observation of the T_g of a minor component in the blend.

The DSC data for the blends are listed in Table II. Glass transition temperatures before and after decomplexation are shown in Figure 7. Although the behavior of the blends containing a large amount of pNECMM is qualitatively similar to that described in ref 37, this is not the case for the low donor content blends. It was previously concluded that pNECMM and pDNBEM were miscible in all proportions when the presence of a single T_g was used as a criterion for miscibility. The blends we prepared containing 15 and 32 mol % of polydonor are clearly two-phase systems, since they exhibit two T_gs. A study of the thermal properties of pNECMM/pDNBEM blends has already shown that the behavior of this system does depend on the molecular weight of the components.[38] The molecular weights of our homopolymers are higher than those in any of the previous investigations, and there is a 3-fold difference in the molecular weights of the two components. There does not appear to be a simple correlation between polymer molecular weight and the formation of electron donor–acceptor complexes. For example, at low donor molecular weights, chain extension may occur rather than network formation; entanglements in very high molecular weight systems could hinder the complexation process and result in increasing incompatibility.[38] Therefore, a variation in the behavior of our samples, and others of a different molecular weight, is likely.

As expected, the miscible blends we prepared have T_gs above the weighted average of the two components.[37] This has been attributed to a decrease in mobility or a reduced free volume as a result of the CT interactions.[39] This effect was also observed for the NECMM–DNBEM random copolymers.[29] It is of interest to compare the effect of CT interactions in the blends to that in the copolymers.

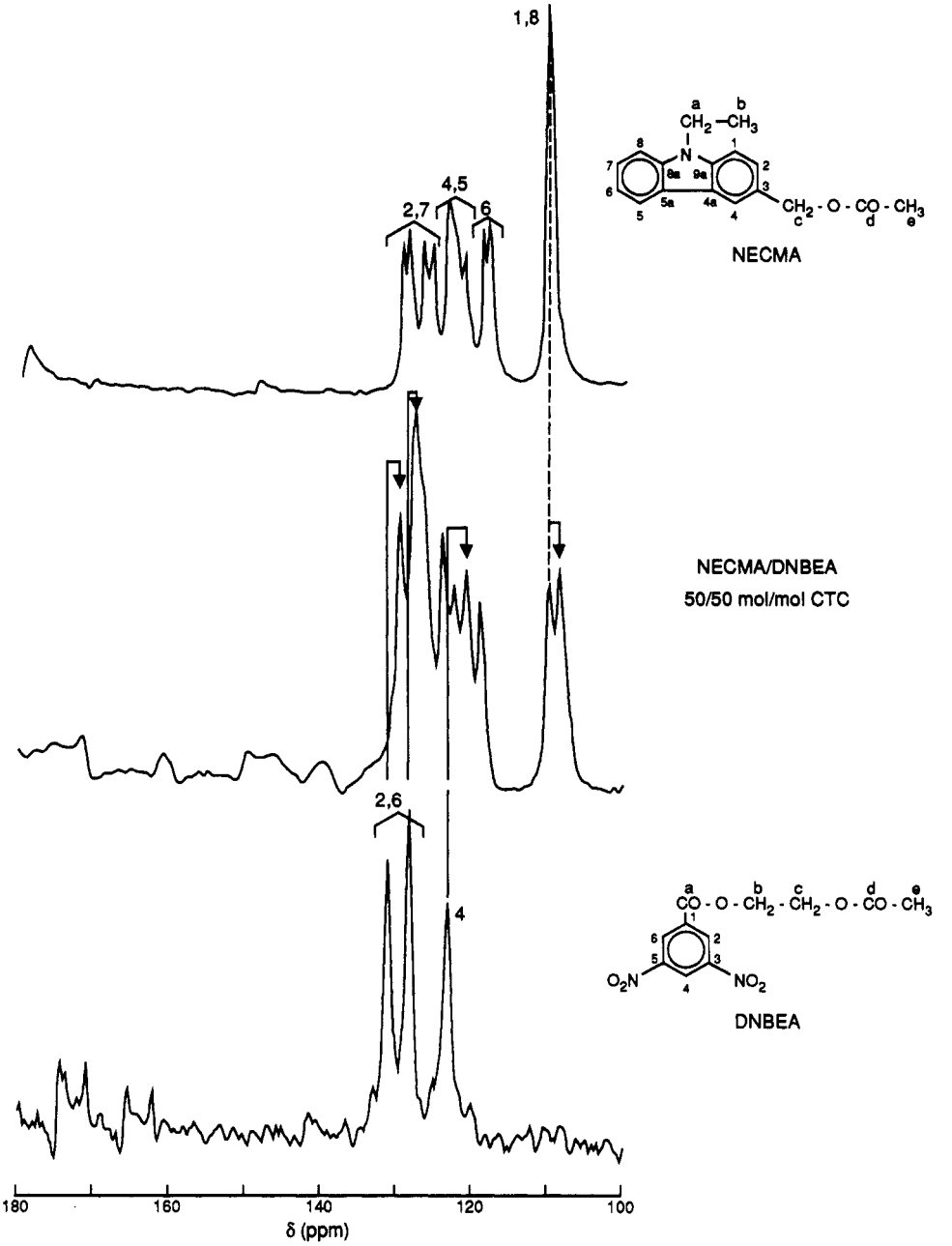

Figure 4. Protonated spectra of samples described in Figure 2 obtained by subtracting dephased spectra in Figure 3 from standard spectra in Figure 2. Arrows indicate shifts due to CTC formation.

Therefore, for each composition, the difference between the weighted average of the homopolymer T_gs and the observed blend or copolymer T_gs was calculated. Figure 8 shows that the copolymer T_gs are increased more by CT interactions than the corresponding miscible blends. This may reflect the presence of both intramolecular and intermolecular complexation in the copolymers, while only intermolecular interactions can be present in the blends.

Comparison to the copolymer T_gs cannot really be made for the two-phase blends, that is for blends containing less than ~35 mol % pNECMM. In these systems, one T_g close to the weighted average and one much higher T_g are seen. At present, the composition of the two phases cannot be determined.

An evaluation of the ΔH values observed upon decomplexation can give us a further understanding of the effect of interactions in these blends. The first time the sample is heated above 185 °C, an endotherm is observed; when the sample is cooled and the experiment repeated with the same sample, a smaller peak is obtained. It has been suggested[38] that the enthalpy change associated with the first endotherm is equal to the enthalpy of decomplexation of the one-phase CT complex and the formation of a system composed of nearly pure donor and acceptor phases. The second endotherm is said to be due to decomplexation of the CTC at the interface of the two domains, and therefore, the difference between the intensity of the first and second endotherms reflects the energy sufficient to convert the two-phase system into a miscible one.[38] Thus, one expects a maximum ΔH for the first scan at a composition of 50/50 pNECMM/pDNBEM, as reported in ref 37.

Figure 9 shows that our results do fit this pattern, but our data are not symmetrical about the 50 mol % pNECMM blend. The deviation from symmetry occurs at the same point that the system becomes phase separated, around 35 mol % NECMM. From the differences between the first and second scans, it appears to be very easy to form a one-phase system when an excess of donor units is present. The large enthalpy of decomplexation observed for the high acceptor content samples may reflect the formation of higher order complexes in one phase, but

Table I
Chemical Shifts of Models Alone Compared to Those in the 1:1 Charge-Transfer Complex (CTC)

carbon	δ, ppm	δ_{CTC},[a] ppm	$\delta_{CTC} - \delta$,[a] ppm
		DNBEA	
d	171.0	171.0 (OL)	(OL)
a	162.2	159.6	−2.6
3, 5	148.9	145.6, 143.4	−3.3, −5.5
1	132.6	127.5 (OL)	−5.1 (OL)
2, 6	131.1, 128.4	128.9, 126.6	−2.2, −1.8
4	123.2	120.1	−3.1
b	66.1	66.4 (OL)	(OL)
c	62.2	60.9	−1.3
e	20.9	19.6 (OL)	(OL)
		NECMM	
d	171.0	171.0 (OL)	(OL)
8a, 9a	140.0	140, 138.4	0, −1.6
2, 7	129.2, 128.3	(OL)	(OL)
	126.4, 125.3	(OL)	(OL)
3	127.7, 125.9	127.4, 125.9	0.3, 0.0
4, 5	123.1, 120.9	123.1, (OL)	0, (OL)
4a, 5a	122.7, 122.1	122.4, 119.4	0.3, −2.7
6	118.4, 117.6	118.4	
1, 8	109.7	109.4, 107.8	0.3, −1.9
c	67.0	66.7 (OL)	(OL)
a	37.0	36.9	−0.1
e	19.1, 18.3	19.7 (OL)	(OL)

[a] (OL), overlap with resonance from other component.

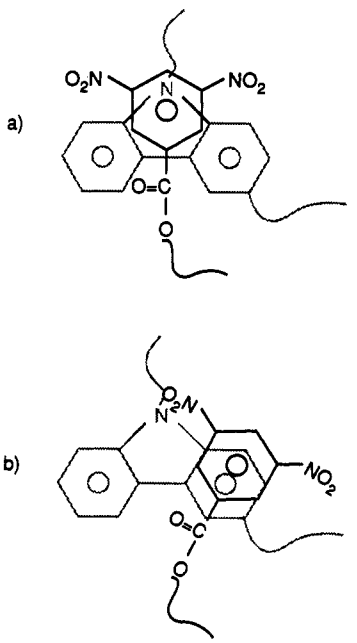

Figure 5. Possible structures for the NECMA/DNBEA CTC. Top: symmetrical structure. Bottom: asymmetrical structure.

since the initial composition of the phases is not known, this is only speculation at this time. It seems unlikely, however, that the higher T_g results from a pNECMM-rich phase, since pNECMM is the minor component. Certainly both the enthalpy of decomplexation and the difference between the first scan and second scan ΔH values seem to be unusually large for high pDNBEM content systems. This would also be consistent with the formation of higher order CTCs in acceptor-rich blends.

(b) NMR Relaxation Studies. We have already shown how changes in the chemical environment of a given nucleus upon mixing two polymers or their small molecule analogues can reveal how the molecules interact in the solid state. Nuclear relaxation can give information about the effect of the CT interactions on the motions of the polymer chain or parts thereof. The relaxation efficiency depends on the extent to which motion at the observation frequency contributes to the distribution of correlation times, and on molecular proximity in the blend.

The parameter we chose to examine in this blend system is the proton spin–lattice relaxation time constant in the rotating frame, $T_{1\rho}(^1H)$. This value is really a measure of spin diffusion between protons. It is a probe of motions in the slow kilohertz range; as such, we believe that it might be more directly comparable to the T_g data discussed above than would T_1, which is sensitive to motion in the megahertz range. The efficiency of spin diffusion is related to the strength of coupling between protons, which depends strongly on the distance between them. Therefore it is a measure of both mobility and molecular proximity, so is ideal for a study of mixing in polymer blends.

Proton $T_{1\rho}$ was measured by use of a pulse sequence with variable contact time, which allowed us to observe the rate of increase of ^{13}C magnetization at short contact times, and the $T_{1\rho}(^1H)$ at long contact times.[12]

Fortunately, there are some resonances in the blends that come only from the pNECMM, and some that come only from the pDNBEM. Therefore, we can measure the $T_{1\rho}(^1H)$ of each component of the blends. This requires a smaller difference in relaxation times to perceive them as separate than by a nonexponential decay of the magnetization. The peaks used for calculation of $T_{1\rho}(^1H)$ are shown in Figure 1, labeled D for the donor (pNECMM) and A for the acceptor (pDNBEM). Details of the procedure are given in a previous paper.[29]

The proton $T_{1\rho}$ values for blends of pNECMM with pDNBEM before and after decomplexation are shown in Figure 10. Table III lists the $T_{1\rho}(^1H)$ values for the pNECMM/pDNBEM blends.

In the past, a common $T_{1\rho}(^1H)$ for the components of a blend was taken to indicate mixing at the molecular level. Nonexponential magnetization decays were used to demonstrate that a system was phase separated. Caution must be used when exponential decays are interpreted as evidence of good mixing. Even when a significant difference in relaxation time constants was detected in our blends by measuring two peaks from each component, a peak containing contributions from both pNECMM and pDNBEM, which we have labeled D + A in Figure 1, appeared to decay exponentially. This is certainly because the differences in $T_{1\rho}$ were less than a factor of 2, but in the absence of nonoverlapping peaks would have led to the erroneous conclusion that molecular mixing was present.

Figure 10 shows that both components of the blends have the same $T_{1\rho}$ before decomplexation. The relaxation times are lower than the weighted average of the two components, indicating that spin diffusion is more efficient in the blends. This reflects a decreased mobility or increased molecular proximity as a result of the reduced free volume in the presence of intermolecular CT interactions. Therefore, $T_{1\rho}(^1H)$ is a measure of interaction between the two types of chains in the same way as T_g is.

Even the blends that possess two T_gs before decomplexation, and must therefore be phase separated, only show one $T_{1\rho}$. This was unexpected, since nuclear relaxation should be sensitive to smaller heterogeneities than T_g is. However, the detection of two phases with similar $T_{1\rho}$ values by our measurements is really only possible if most or all of one component is found in one phase. There is no observable difference in chemical shift between pDNBEM in one phase and pDNBEM in a second phase of a different composition. As a result, the $T_{1\rho}$ calculated is an average of more than one value, unless the difference in relaxation in the two phases is so great that a nonexponential decay is observed. The detection of only one $T_{1\rho}$ for a system with two T_gs may suggest that the phases are not primarily pDNBEM or pNECMM, but that both

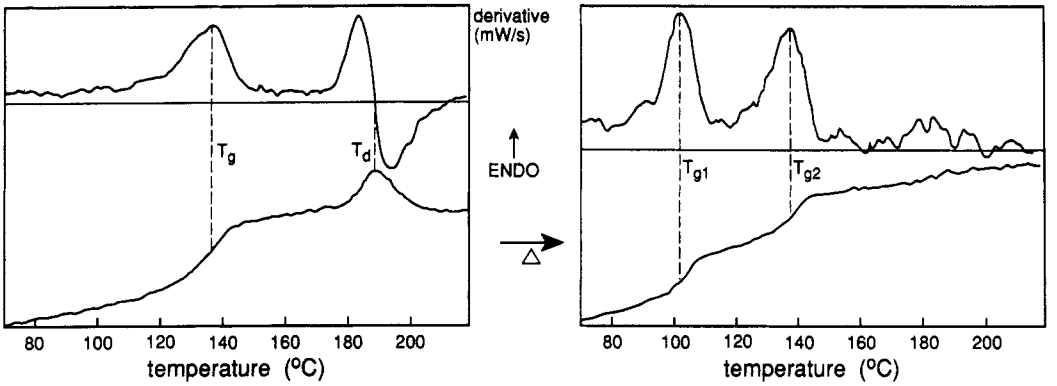

Figure 6. DSC heating scan data for a 50:50 (mol/mol) blend of pNECMM and pDNBEM (bottom) with the first derivative (top). On the left are the data obtained the first time the sample is heated above 185 °C, which results in decomplexation; on the right are data obtained on a previously decomplexed sample.

Table II
Thermal Data for pNECMM/pDNBEM Blends

mol % NECMM	T_g, °C before heating	T_g, °C after heating	ΔH, J/g first scan	ΔH, J/g second scan
0.0	102	97		
15.0	107, 127	99, 130	1.7	2.0
31.6	114, 127	101, 137	2.0	0.1
50.0	136	102, 138	3.4	0.0
70.0	141	110, 139	2.3	1.5
85.0	139	?, 139	0.9	0.5
100.0	140	140		

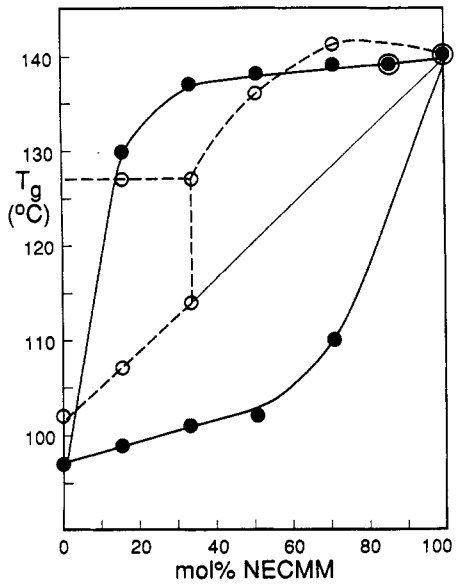

Figure 7. Glass transition temperature vs composition for pNECMM/pDNBEM blends. ○, before decomplexation; ●, after decomplexation.

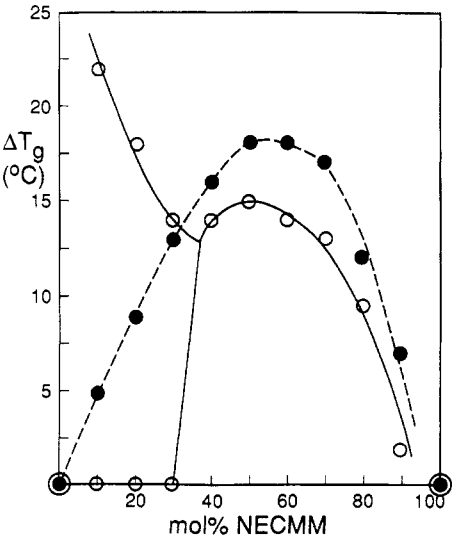

Figure 8. Difference between observed T_g and the weighted average of component T_gs vs composition for pNECMM/pDNBEM blends (○) and NECMM–DNBEM copolymers (●).

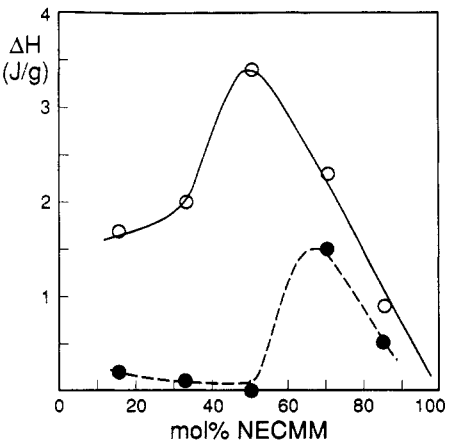

Figure 9. Enthalpy changes for pNECMM/pDNBEM blends from DSC vs composition. ○, first scan above 185 °C; ●, subsequent scan.

phases contain some CTC. One phase may contain 1:1 CTC, while another may have higher order complexes. The interproton distances in each phase may be similar and lead to comparable relaxation rates. This would also be consistent with the high ΔH of decomplexation and the observed T_g values for the two-phase systems discussed earlier.

Figure 10 also shows the $T_{1\rho}$s for the pNECMM/pDNBEM blends after decomplexation has occurred. Two $T_{1\rho}$s were found for the decomplexed blends if enough of one component was present to produce a sufficiently intense peak. The DSC data suggest that essentially pure polydonor and polyacceptor phases are formed on decomplexation. The lower $T_{1\rho}$ for the decomplexed blends seems to be comparable to that of pDNBEM. However, in contrast to the T_g behavior, the higher $T_{1\rho}$ value never reaches that of pNECMM. pNECMM in the decomplexed blends may have more efficient spin diffusion than in the homopolymer due to CTC formation at the interface with the pDNBEM phase. This would result in some protons being closer than in the pNECMM, and they would relax faster and dominate the relaxation behavior.

Figure 11 shows the relative decrease in $T_{1\rho}(^1H)$ for the copolymers, taken from ref 29, and the blends. Just as the T_gs of the copolymers are higher than those of the blends, the $T_{1\rho}$s of the copolymers show a stronger

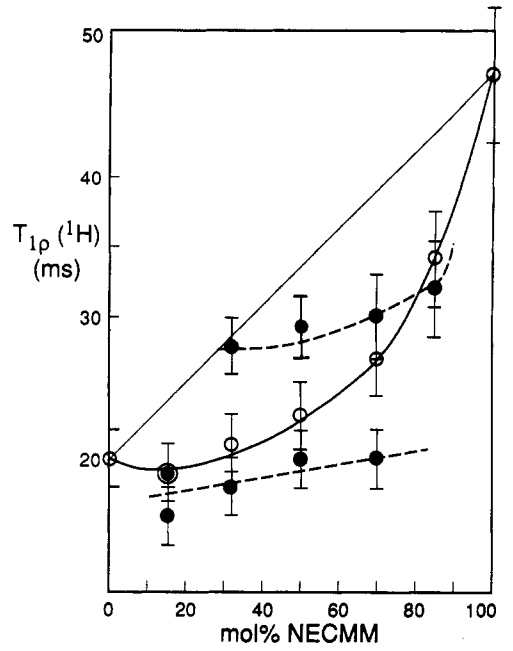

Figure 10. $T_{1\rho}(^1H)$ vs composition for pNECMM/pDNBEM blends. O, before complexation; ●, after decomplexation.

Table III
$T_{1\rho}(^1H)$ for pNECMM/pDNBEM Blends before and after Decomplexation

mol % NECMM	$T_{1\rho}(^1H)$, ms: before heating to 195 °C	$T_{1\rho}(^1H)$, ms: after heating to 195 °C
0.0	20	19
15.0	19	16, 19
31.6	21	18, 28
50.0	23	19, 29
70.0	27	20, 30
85.0	34	?, 32
100.0	47	47

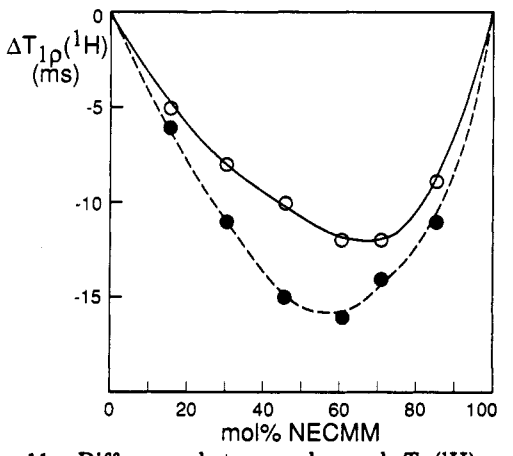

Figure 11. Difference between observed $T_{1\rho}(^1H)$ and the weighted average of the components vs composition. O, pNECMM/pDNBEM blends; O, NECMM-DNBEM copolymers.

depression than do those of the blends. Both observations are consistent with a greater restriction of mobility or reduction in free volume in the copolymers. It appears that the covalent bonding of donor and acceptor groups results in stronger interactions and a greater average proximity of the interacting groups in the copolymers than in the blends.

Homopolymer/Copolymer Blends. In order to introduce varying amounts of intramolecular CT interactions into the blend system under consideration, a number of homopolymer/copolymer blends were prepared. Three NECMM-DNBEM copolymers, one donor-rich, one approximately 1:1 donor/acceptor, and one acceptor-rich were prepared simultaneously with the homopolymers. The T_g and $T_{1\rho}$ values for these blend components are given in Table IV. In general, their properties followed the trends already reported for copolymers of NECMM with DNBEM.[29] Blends were prepared as for the homopolymer blends described above. Blends with four different NECMM to DNBEM ratios were made from each copolymer by adding the required amount of homopolymer. They were subjected to the same DSC and solid-state NMR analysis as the homopolymer blends.

Table IV
Properties of Homopolymers and Copolymers Used To Prepare Blends

sample	T_g, °C: before heating	T_g, °C: after heating	$T_{1\rho}(^1H)$, ms: before heating	$T_{1\rho}(^1H)$, ms: after heating
pDNBEM	102	97	20	19
N329[a]	125	119	22	
N549[a]	140	136	23	
N731[a]	146	143	25	
pNECMM	140	140	47	47

[a] NECMM-DNBEM copolymers designated N*xxx* where *xxx* indicates mole percent NECMM in copolymer. (e.g., N329 contains 32.9 mol % NECMM).

Table V
Thermal Data for Homopolymer/Copolymer Blends

mol % NECMM	CP,[a] wt %	HP,[b] wt %	T_g, °C: before heating	T_g, °C: after heating	ΔH, J/g: first scan	ΔH, J/g: second scan
15	N329 44.8	pDNBEM 55.2	111	105	0.6	0.3
15	N549 26.3	pDNBEM 73.7	111	103	0.0	
15	N731 19.4	pDNBEM 80.6	110, 126	101, 137	0.3	0.0
30	N329 90.0	pDNBEM 9.1	122	15		0.0
30	N549 53.3	pDNBEM 46.7	117, 125	103, 129	0.0	0.2
30	N731 39.3	pDNBEM 60.7	115, 125	102, 140	0.8	0.5
50 75.8	N329 24.2	pNECMM	133	122, 137	0.9	0.0
50	N549 90.6	pDNBEM 9.4	139	133	0.2	
50	N731 66.8	pDNBEM 33.2	139	112, 140	1.0	0.5
70	N329 46.4	pNECMM 53.6	141	124, 137	1.6	0.1
70	N549 67.5	pNECMM 32.5	144	139	0.0	0.2
70	N731 95.5	pDNBEM 4.5	146	143	0.0	0.2

[a] CP, copolymer. [b] HP, homopolymer.

(a) Thermal Analysis. Table V lists the DSC data for the homopolymer/copolymer blends. Figure 12 shows the T_gs of the blends before decomplexation. In many respects the behavior of the blends containing copolymers is similar to that of pNECMM/pDNBEM blends. Above ~35 mol % NECMM groups, all the blends have a single T_g, which is greater than the weighted average of the corresponding homopolymer/copolymer pair. Below 35 mol % NECMM, the blends usually possess two T_gs. In the case of blends containing the 32.9 mol % NECMM copolymer, only one T_g was detected, probably because the amount of added pDNBEM was so small, or because the T_gs of the two phases are too similar. When the 54.9 or 73.1 mol % NECMM copolymer is present in the blend, a high-T_g phase, and one that has a T_g at or below the weighted

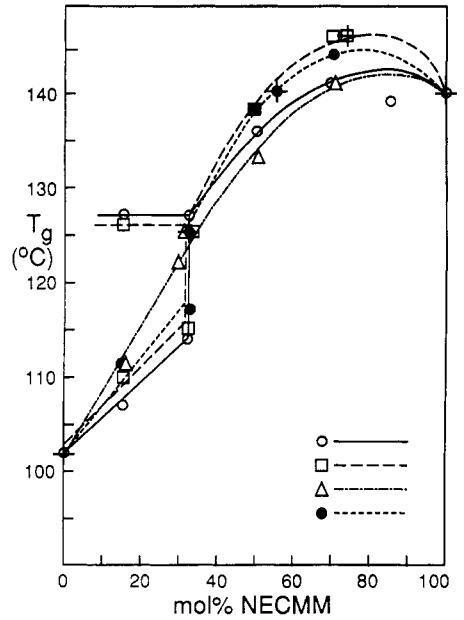

Figure 12. T_g vs composition before decomplexation for copolymer/homopolymer blends described in Table V. Symbols with superimposed + indicate single components. ○, homopolymer blends; △ = blends containing copolymer N371; ●, blends containing copolymer N549, □, blends containing copolymer N731.

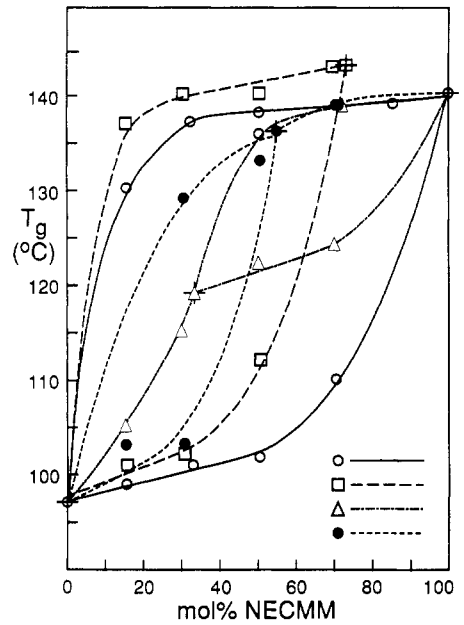

Figure 13. T_g vs composition after decomplexation for homopolymer/copolymer blends described in Table V. Symbols as for Figure 12.

average of the components, are seen. The T_g of the high-T_g phase is similar to that seen in the homopolymer blends. The depression of the lower T_g may reflect a disruption of the intramolecular CT interactions upon formation of the CTC with the added homopolymer.

Figure 13 shows the T_gs of the blends after decomplexation. Two T_gs were observed in the blends whenever sufficient homopolymer was present. Whether the blends contain two homopolymers or a homopolymer and a copolymer, it appears that decomplexation results in the formation of two essentially pure phases of the starting components.

Table V shows that the ΔHs of decomplexation values exhibit a slightly different trend depending on whether the blend contains only homopolymers (Table II) or a copolymer and a homopolymer. The maximum ΔH is no longer at a composition of 1:1 DNBEM to NECMM units in the copolymer-containing blends. Instead it reaches a maximum somewhere between the copolymer composition and the pure homopolymer. Indeed, it approaches zero when only one component, whether homo- or copolymer, is present.

Table VI
$T_{1\rho}(^1H)$ for Homopolymer/Copolymer Blends

mol % NECMM	CP,[a] wt %	HP,[b] wt %	$T_{1\rho}$, ms before heating	$T_{1\rho}$, ms after heating
30	N329 90.9	pDNBEM 9.1	23	17
30	N549 53.3	pDNBEM 46.7	21	18
30	N731 39.3	pDNBEM 60.7	20	18,22
50	N329 75.8	pNECMM 24.2	23	20
50	N549 90.6	pDNBEM 9.4	20	
50	N731 66.8	pDNBEM 33.2	21	23
70	N329 46.4	pNECMM 53.6	26	20,30

[a] CP, copolymer. [b] HP, homopolymer.

The position of the ΔH maximum depends both on the actual ratio of donor to acceptor groups and on the proportion of added homopolymer in the copolymer/homopolymer blends, that is, on how much interaction is not accounted for in the copolymer. This is exactly the pattern expected for the number of intermolecular contacts. This confirms that decomplexation only involves intermolecular CTCs and that CTCs formed intramolecularly are not pulled apart. This accounts for the absence of a decomplexation endotherm in the copolymers.[29] The ΔH values for the heating of the already decomplexed copolymer/homopolymer blends are all very small and do not show a recognizable pattern. This seems to indicate a reduced amount of interfacial CT complexation. When phase separation occurs, the copolymer is free to assume the optimum conformation that maximizes intramolecular CT complexation. Apparently this leaves fewer interacting groups available at the interface than are present in the homopolymer blends.

(b) NMR Relaxation Studies. Table VI lists the NMR relaxation data for a number of homopolymer/copolymer blends. These blends have $T_{1\rho}(^1H)$ values lower than the weighted average of their constituents. Figure 14 shows that the $T_{1\rho}$s of the copolymer-containing blends are the same as those of the homopolymer blends within the margin of error of our determinations. In addition, all the copolymer/homopolymer blends tested had one $T_{1\rho}$ for both donor units and acceptor units. The efficiency of spin diffusion in the blends is, therefore, comparable whether they are composed only of homopolymers or whether a copolymer is present. This suggest that the minimum interproton distance in the copolymer-containing blends is similar to that in the homopolymer blends.

The nuclear relaxation of some decomplexed copolymer/homopolymer blends was investigated. Table V reveals that sometimes a single $T_{1\rho}$ was observed in copolymer-containing blends whereas the corresponding homopolymer blends exhibit two $T_{1\rho}$s, and that the pattern of $T_{1\rho}$ values is not as clear as in the homopolymer blends. This results from an inherent sensitivity problem with this method: it does not distinguish between magnetization arising from NECMM in the homopolymer and from NECMM in a copolymer or mixed phase. There would

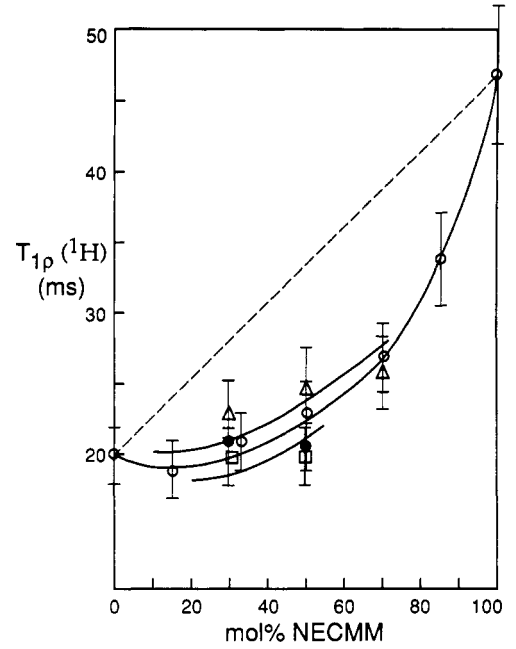

Figure 14. $T_{1\rho}(^1H)$ vs composition before decomplexation for homopolymer/copolymer blends described in Table VI. Symbols as for Figure 12.

have to be a difference in chemical shift so the relaxation in each environment could be measured separately. Alternatively, a much larger difference in relaxation rates in the homopolymer and the copolymer would have to be present to detect a nonexponential decay. In the samples analyzed, a short $T_{1\rho}$, similar to the lower one observed for the homopolymer blends, was seen, and sometimes a longer $T_{1\rho}$, lower than that of the pure copolymer, was also detected. This can be accounted for by the fact that only the average $T_{1\rho}$ for a NECMM or DNBEM unit can be determined, as discussed above.

Conclusions

This investigation has shown that solid-state NMR can be used to get information about the effect of CT interactions in bulk polymers, and that its results can be correlated with data about macroscopic properties obtained by DSC. Changes in chemical shift resulting from CT complexation in small molecule analogues are consistent with an asymmetrical structure for the complex. Blends were found to be two-phase systems below ~35 mol % NECMM units. Data suggest that both phases contain some CTC, perhaps with higher order CTCs being formed. At higher NECMM contents, miscible blends are formed. Both DSC and NMR relaxation in the solid state reveal a decrease in mobility and a reduction in free volume due to the CT interactions.

Upon being heated above ~185 °C, the blends separate into two phases. Both homopolymer and copolymer blends undergo essentially complete separation into the blend components. Thermal behavior of the copolymer/homopolymer blends confirms that only intermolecular CTCs are affected during decomplexation.

Acknowledgment. We thank the Natural Science and Engineering Research Council of Canada and the Ontario Centre for Materials Research for financial support.

References and Notes

(1) Cruz-Ramos, C. A.; Paul, D. R. *Macromolecules* **1989**, *22*, 1289.
(2) Kim, J. H.; Barlow, J. W.; Paul, D. R. *J. Polym. Sci., Part B: Polym. Phys.* **1989**, *27*, 223.
(3) Clavreul, R.; Bloch, B.; Brigodiot, M.; Marechal, E. *Makromol. Chem.* **1987**, *188*, 67.
(4) Attias, A. J.; Ancelle, J.; Bloch, B.; Laupretre, F. *Polym. Bull.* **1987**, *18*, 217.
(5) Komoto, T.; Ando, I.; Nakamoto, Y.; Ishida, S. *J. Chem. Soc., Chem. Commun.* **1988**, 135.
(6) Lee, F.; Gabe, E.; Tse, J. S.; Ripmeester, J. A. *J. Am. Chem. Soc.* **1988**, *110*, 6014.
(7) Blann, W. G.; Fyfe, C. A.; Lyerla, J. R.; Yannoni, C. S. *J. Am. Chem. Soc.* **1981**, *103*, 4030.
(8) Grobelny, J.; Rice, D. M.; Karasz, F. E.; MacKnight, W. J. *Macromolecules* **1990**, *23*, 2139.
(9) Belfiore, L. A.; Lutz, T. J.; Cheng, C.; Bronnimann, C. E. *J. Polym. Sci., Part B: Polym. Phys.* **1990**, *28*, 1261.
(10) Natansohn, A. *Macromolecules* **1991**, *24*, 1662.
(11) Stejskal, E. O.; Schaefer, J.; Sefcik, M. D.; McKay, R. A. *Macromolecules* **1981**, *14*, 188.
(12) Stejskal, E. O.; Schaefer, J.; Sefcik, M. D.; McKay, R. A. *Macromolecules* **1981**, *14*, 275.
(13) Tekely, P.; Laupretre, F.; Monnerie, L. *Polymer* **1985**, *26*, 1081.
(14) Grinsted, R. A.; Koenig, J. L. *J. Polym. Sci., Part B: Polym. Phys.* **1990**, *28*, 177.
(15) Dickinson, L. C.; Yang, H.; Chu, C. W.; Stein, R. S.; Chien, J. C. W. *Macromolecules* **1987**, *20*, 1757.
(16) Henrichs, P. M.; Tribone, J.; Massa, D. J.; Hewitt, J. M. *Macromolecules* **1988**, *21*, 1282.
(17) Chu, C. W.; Dickinson, L. C.; Chien, J. C. W. *Polym. Bull.* **1988**, *19*, 265.
(18) Parmer, J. F.; Dickinson, L. C.; Chien, J. C. W.; Porter, R. S. *Macromolecules* **1989**, *22*, 1078.
(19) Zhang, X.; Wang, Y. *Polymer* **1989**, *30*, 1867.
(20) Natansohn, A.; Lacasse, M.; Banu, D.; Feldman, D. *J. Appl. Polym. Sci.* **1990**, *40*, 899.
(21) Grobelny, J.; Rice, D. M.; Karasz, F. E.; MacKnight, W. J. *Polym. Commun.* **1990**, *31*, 86.
(22) Marco, C.; Fatou, J. G.; Gomez, M. A.; Tanaka, H.; Tonelli, A. E. *Macromolecules* **1990**, *23*, 2183.
(23) Parizel, N.; Laupretre, F.; Monnerie, L. Third European Symposium on Polymer Blends, July 1990; p B21.
(24) Spevacek, J.; Schneider, B.; Straka, J. *Macromolecules* **1990**, *23*, 3042.
(25) Liu, Y.; Roy, A. K.; Jones, A. A.; Inglefield, P. T.; Ogden, P. *Macromolecules* **1990**, *23*, 968.
(26) Sultany, K. *Polym. Bull.* **1988**, *20*, 463.
(27) Huijgen, T. P.; Gaur, H. A.; Weeding, T. L.; Jenneskens, L. W.; Schuurs, H. E. C.; Huysmans, W. G. B.; Veeman, W. S. *Macromolecules* **1990**, *23*, 3063.
(28) Natansohn, A.; Simmons, A. *Macromolecules* **1989**, *22*, 4426.
(29) Simmons, A.; Natansohn, A. *Macromolecules* **1990**, *23*, 5127.
(30) Simionescu, C. I.; Percec, V. *J. Polym. Sci., Polym. Chem. Ed.* **1979**, *17*, 2287.
(31) Simionescu, C. I.; Percec, V.; Natansohn, A. *Polym. Bull.* **1980**, *3*, 535.
(32) Percec, V.; Natansohn, A.; Simionescu, C. I. *Polym. Bull.* **1981**, *4*, 255.
(33) Natansohn, A. *J. Polym. Sci., Polym. Chem. Ed.* **1984**, *22*, 3161.
(34) Opella, S. J.; Frey, M. H. *J. Am. Chem. Soc.* **1979**, *101*, 5854.
(35) Brimacombe, L.; Natansohn, A. *J. Appl. Polym. Sci.* **1990**, *40*, 1063.
(36) Pearson, J. M.; Turner, S. R.; Ledwith, A. *Molecular Associations*; Foster, R., Ed.; Academic Press: New York, 1979; Vol. 2, p 79.
(37) Rodriguez-Parada, J. M.; Percec, V. *Macromolecules* **1986**, *19*, 55.
(38) Pugh, C.; Rodriguez-Parada, J. M.; Percec, V. *J. Polym. Sci., Part A: Polym. Chem.* **1986**, *24*, 747.
(39) Epple, U.; Schneider, H. A. *Thermochim. Acta* **1990**, *160*, 103.

Registry No. *p*NECMM (homopolymer), 67549-45-5; *p*DNBEM, 82008-07-9; NECMA, 67549-44-4; DNBEA, 78198-10-4; NECMA·DNBEA, 122624-69-5; (NECMM)(DNBEM) (copolymer), 122624-70-8.